Unusual Four-Bond Secondary H/D Isotope Effect Supports a Short−Strong Hydrogen Bond between Phospholipase A₂ and a Transition State Analogue Inhibitor[†]

Chunhua Yuan,[‡,§] Shengjiang Tu,[‡] Michael H. Gelb,[#] and Ming-Daw Tsai*,[‡,§,||,⊥]

Departments of Chemistry and Biochemistry and Campus Chemical Instrument Center, The Ohio State University, Columbus, Ohio 43214, Genomics Research Center, Academia Sinica, Taipei, Taiwan, and Departments of Chemistry and Biochemistry, University of Washington, Seattle, Washington 98195

ABSTRACT: A prominent secondary four-bond hydrogen/deuterium isotope effect was observed from proton NMR at the active site histidine imidazole ring of bovine pancreatic sPLA₂ in the presence of a phosphonate transition state analogue. The cross-modulation of $H^{\epsilon 2}$/H48 and $H^{\delta 1}$/H48 resonances was confirmed by line shape simulation that follows the McConnell equation with fractionation factors incorporated to account for the change in the signal magnitude as well as the resonance line shape at various H_2O/D_2O solvent mixtures. While the downfield shift of each individual proton upon deuteration on the opposite site can be attributed to the proton-relay system of the H48-D99 catalytic dyad in sPLA₂, the observation that $H^{\delta 1}$/H48 induces a 3-fold larger H/D secondary isotope effect (∼0.15 ppm) on $H^{\epsilon 2}$/H48 than vice versa (∼0.05 ppm) is interpreted as additional spectroscopic evidence for the previously proposed short−strong hydrogen bond formed between the donor $N^{\delta 1}$/H48 and a nonbridging phosphonate oxygen atom of the transition state analogue. These results provide additional details for the catalytic mechanism of sPLA₂ and demonstrate that the intrinsic H/D secondary isotope effect is a useful tool to probe hydrogen bond strength.

Bovine pancreatic secreted phospholipase A₂ (sPLA₂)[1] is a calcium-dependent lipolytic enzyme that catalyzes the hydrolysis of the 2-acyl ester bond of 3-*sn*-phosphoglycerides (*1*). The enzyme employs an Asp-His (D99-H48) pair together with a conserved water molecule as the catalytic triad that mimics the Asp-His-Ser triad in serine proteases. Following the work of low-barrier hydrogen bonds (LBHB) on serine proteases (*2*, *3*), though its existence is under intensive debate (*4*), NMR investigation has been conducted recently on sPLA₂. The study led to detection of a downfield proton signal around 18 ppm, a characteristic resonance of LBHB, in the presence of a phosphonate transition state analogue (TSA) (*5*, *6*). The peak was then rigorously assigned to $H^{\delta 1}$/H48 that bridges H48 and the transition state analogue, which differs from the LBHB formation site between the Asp and His residues of the catalytic triad in serine proteases, perhaps due to the use of a different lone
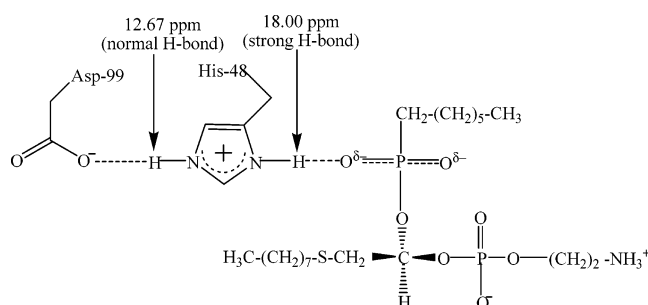

FIGURE 1: Schematic diagram showing a normal hydrogen bond between D99 and H48 and a strong hydrogen bond between H48 and TSA involving bridging atoms $H^{\epsilon 2}$ and $H^{\delta 1}$ of H48, respectively.

pair of the Asp carboxylate side chain (anti lone pair in sPLA₂s vs syn lone pair in serine proteases) in the Asp−His hydrogen bond (*6*). Several distinctive physicochemical features commonly associated with LBHB (*3*, *7*) have also been observed except that evidence is lacking for the most important criterion: the bond strength, i.e., >10 kcal/mol. Nevertheless, this intermolecular hydrogen bond with a bond strength likely in the range of 4.5−8 kcal/mol estimated from the pK_a determination (*6*) and inhibition kinetic studies (*8*) could be regarded as one of the stronger hydrogen bonds that contribute to the transition state stabilization (*3*, *6*, *9*).

In contrast, the hydrogen bond between $N^{\epsilon 2}$/H48 and the carboxylate side chain of D99 is considered as normal type based on the chemical shift of the bridging proton (Figure 1). Since the $H^{\epsilon 2}$/H48 resonance also appears in the well-resolved downfield region recorded on the sPLA₂−TSA

* To whom correspondence should be addressed at the Department of Chemistry, The Ohio State University, 100 West 18th Ave., Columbus, OH 43210-1173. Telephone: (614) 292-3080. Fax: (614) 292-1532. E-mail: tsai.7@osu.edu.
‡ Department of Chemistry, The Ohio State University.
§ Campus Chemical Instrument Center, The Ohio State University.
# University of Washington.
|| Department of Biochemistry, The Ohio State University.
⊥ Genomics Research Center, Academia Sinica.

1 Abbreviations: LBHB, low-barrier hydrogen bond; NMR, nuclear magnetic resonance; ppm, parts per million; sPLA₂, secreted phospholipase A₂; TSA, transition state analogue.
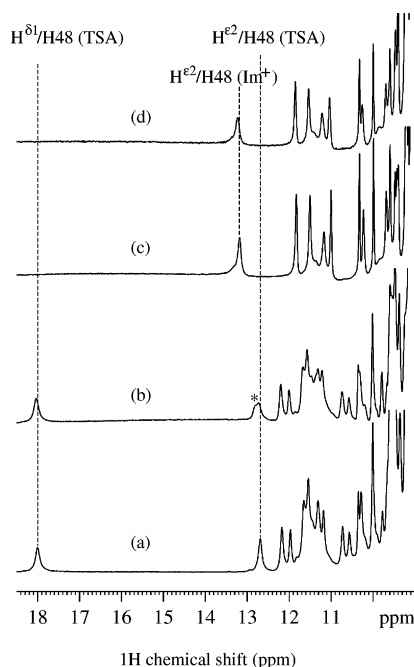
FIGURE 2: (a) Downfield region of the ^{1}H NMR spectrum acquired on the sPLA$_2$−TSA complex in 90% H$_2$O and 10% D$_2$O. The two distinct peaks at 12.67 and 18.00 ppm have been unambiguously assigned to H$^{\epsilon 2}$ and H$^{\delta 1}$ of H48, respectively, via site-directed mutagenesis and specific isotope labeling (6). (b) The asterisk indicates the doublet splitting of H$^{\epsilon 2}$/H48 in the fractionation factor experiments when the deuterium content of the solvent reaches 60 vol %. (c) 1D ^{1}H NMR spectrum acquired on the free sPLA$_2$ at pH 4.7 dissolved in 90% H$_2$O and 10% D$_2$O. Under such acidic condition H48 exists in an imidazolium form, and H$^{\epsilon 2}$/H48 appears around 13.1 ppm. (d) 1D ^{1}H NMR spectrum acquired on the free sPLA$_2$ at pH 4.7 dissolved in 40% H$_2$O and 60% D$_2$O. No splitting can be observed for the H$^{\epsilon 2}$/H48 resonance. All of the data were collected at 285 K using jump−return to suppress water signal.

complex (Figure 2), comparison of physicochemical properties such as hydrogen/deuterium isotope effects between H$^{\delta 1}$/H48 and H$^{\epsilon 2}$/H48 can provide more insight into the nature of the H48-mediated hydrogen-bonding network in the complex. There is a growing list of experimental evidence that H/D isotope effects are good diagnostic properties of hydrogen bond strength (10−14). Isotope effects on chemical shifts are defined as $^n\Delta^m X(YI) = \delta X(I_{\text{light}}) - \delta X(I_{\text{heavy}})$, where m is the mass of the isotope I, n is the number of bonds between the isotope and the reporter nucleus X, and Y is the nucleus to which the isotope is attached (15). In general, the magnitude of $^n\Delta^m X(YI)$ increases with the range of the chemical shifts of the reporter nucleus but falls off rapidly with the number of bonds.

In this work we performed detailed analysis of the H/D fractionation factors and secondary isotope effects of these two protons. The results delineate a more widened (lower fractionation factor) and more anharmonic (larger secondary isotope effect) vibrational potential of H$^{\delta 1}$/H48 with respect to that of H$^{\epsilon 2}$/H48, which in turn strengthens the previous proposition of a stronger hydrogen bond between H48 and TSA involving H$^{\delta 1}$/H48 and provides further insight into the catalytic mechanism of sPLA$_2$. More importantly, the study demonstrates that the secondary isotope effect can serve as a probe of hydrogen bond strength involving a histidine imidazole ring, which plays a significant role in the function of numerous proteins.

MATERIALS AND METHODS

Sample Preparation. Bovine pancreatic sPLA$_2$ was overexpressed in *Escherichia coli* BL21(DE3)[pLysS] cells and purified as described (16). The deuterium fractionation experiment has been described previously (6). Briefly, seven sPLA$_2$−TSA samples were prepared in H$_2$O/D$_2$O mixtures with D$_2$O volume percentages of 10%, 20%, 40%, 50%, 60%, 70%, and 85% in otherwise identical conditions [0.7 mM protein, ∼1 mM inhibitor, pH* 6.0 (uncorrected), 200 mM NaCl, and 50 mM CaCl$_2$]. Parallel fractionation factor experiments were also performed on the free sPLA$_2$ to investigate the behavior of H$^{\epsilon 2}$/H48 in the imidazolium form. The seven samples contained about 0.5 mM protein, 200 mM NaCl, and 50 mM CaCl$_2$ at pH* 4.7 with D$_2$O volume percentages of 10%, 25%, 40%, 50%, 60%, 70%, and 85%, respectively, in the H$_2$O/D$_2$O solvent mixture.

NMR Spectroscopy. One-dimensional proton NMR experiments were carried out at 285 K on a Bruker DMX-600 spectrometer after more than 2 weeks of incubation at room temperature. Water signal suppression was achieved with the jump−return technique (17), with the carrier frequency set on the water signal and the delay between the pulses optimized to achieve maximal excitation at 15 ppm. Each data set was acquired with 8K time domain points, 170 ms acquisition time, 1.0 s relaxation delay, and 20000 scans (∼6.5 h experimental time). The sPLA$_2$−TSA sample with 60% volume percentage of D$_2$O was used to investigate temperature-dependent line shape evolution of the H$^{\epsilon 2}$/H48 resonance. The experimental temperature was calibrated with neat methanol (7).

Data Analysis. NMR data were processed using the XWINNMR software (Bruker Inc.). ^{1}H chemical shifts were referenced to the external standard 2,2-dimethyl-2-silapentane-5-sulfonate (DSS). To extract fractionation factors, the H$^{\epsilon 2}$/H48 and H$^{\delta 1}$/H48 signals at various solvent mixtures were integrated and calibrated against nonexchangeable high-field methyl groups, and the fitting was performed using SigmaPlot 8.0 software (SPSS Inc.). The line shape simulation of both H$^{\delta 1}$/H48 and H$^{\epsilon 2}$/H48 spins in the presence of TSA was carried out using the program Maple (version 7, Waterloo Maple Inc.).

RESULTS AND DISCUSSION

Fractionation Factors of Imidazole NH Protons of H48 in the Presence of TSA. The deuterium/protium fractionation factor measures the preference of deuterium over protium in an exchangeable site with respect to the solvent. A good correlation has been found between the fractionation factor value and hydrogen bond strength; e.g., a short−strong hydrogen bond is characterized by a low fractionation factor (10, 11). To establish the LBHB nature involving the H$^{\delta 1}$/H48 proton, the deuterium fractionation factor ($\phi^{\delta 1} = 0.62$) has been deduced previously from quantitative measurement of the peak intensity as a function of deuterium content followed by nonlinear least-squares regression analysis to the equation (6):
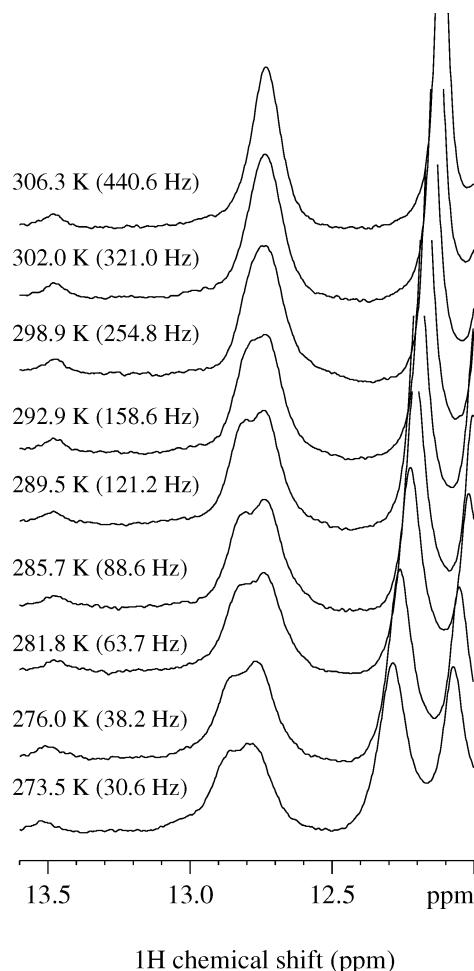
$$I = \frac{I_{\max}x}{\phi(1-x)+x} \quad (1)$$

FIGURE 3: The jump−return experiments performed on the sPLA$_2$−TSA sample with 60% D$_2$O in the solvent mixture reveal a temperature-dependent line shape of the H$^{\epsilon 2}$/H48 resonance (∼12.7 ppm). The experimental temperature and the exchange rate k_{ex} of the H$^{\delta 1}$/48 proton are indicated. The latter was calculated from the following equation: $k_{ex} = \exp(-E_{ex}/RT + C_{ex})$, where E_{ex} and C_{ex} are 13.5 kcal/mol and 28.3, respectively (6). The coalescence point around 292.9 K is explained in the text.

where x is the mole fraction of H$_2$O in the H$_2$O/D$_2$O mixture, I is the peak intensity at a given x, and I_{max} is the maximal intensity when x equals 1.0. In the determination of $\phi^{\epsilon 2}$, however, two relatively well-resolved peaks can be distinguished around 12.74 ppm when the deuterium content of the solvent reaches 50−70 vol % (Figure 2b). By running temperature-dependent line shape experiments on the sample with 60% D$_2$O in the solvent mixture, it was found that the doublet being resolved on the NMR time scale at lower temperature (e.g., 285 K) gradually evolves into one peak at higher temperature (e.g., 304 K) (Figure 3). This observation implicates that the two doublet components are undergoing chemical exchange and thus should be assigned to H$^{\epsilon 2}$/H48 corresponding to two magnetic environments. Therefore, the peak integral was used in eq 1 fitting (Figure 4). To be consistent, $\phi^{\delta 1}$ of H48 was reexamined by integrating the most downfield proton signal (Figure 4). The results support a normal hydrogen bond involving H$^{\epsilon 2}$ ($\phi^{\epsilon 2}$ ∼ 0.95) and a stronger hydrogen bond involving H$^{\delta 1}$ ($\phi^{\delta 1}$ ∼ 0.61) for the active site histidine residue.

Origin of H$^{\epsilon 2}$/H48 Resonance Splitting. The doublet splitting of H$^{\epsilon 2}$/H48 in the complex should be caused by the
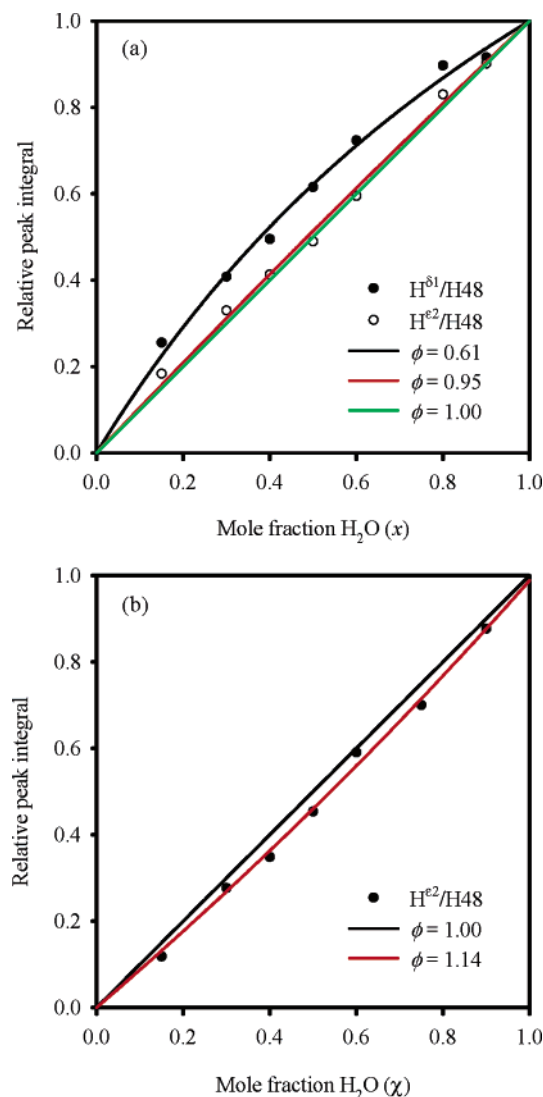

FIGURE 4: (a) Determination of the fractionation factor of H$^{\epsilon 2}$/H48 ($\phi^{\epsilon 2}$) in the presence of TSA. The peak integral from NMR data collected at 285 K was used for the nonlinear least-squares fitting. For comparison, the fractionation factor of H$^{\delta 1}$/H48 was redetermined using the resonance integral, and the result is virtually the same as before (6). (b) Determination of the fractionation factor of H$^{\epsilon 2}$/H48 ($\phi^{\epsilon 2}$) in the absence TSA at pH 4.7, when H48 exists in a protonated form.

H/D isotope effect from a remote labile site. While the shift could be a cumulative effect, structural inspection of the local environment (18) suggests that H$^{\delta 1}$/H48, which is four bonds away and engaged in an intermolecular hydrogen bond, is the most likely major contributor. Two lines of evidence support this origin, and the resulting phenomenon is the experimental manifestation of the secondary isotope effect on chemical shift defined as $^4\Delta^1$H-$\epsilon 2$(N$^{\delta 1}$-D). First, as shown in Figure 5, the relative peak intensities of the doublet apparently change in parallel to H$_2$O/D$_2$O ratios. A close look reveals that the change can be quantitatively correlated to the relative population of H/D at the N$^{\delta 1}$/H48 site. For example, it is expected from $\phi^{\delta 1}$ that protium and deuterium would be equally populated on the N$^{\delta 1}$/H48 site when D$_2$O reaches 62 vol %, and by visual inspection of Figure 5b the doublets are also likely of equal intensity in such a solvent mixture. Second, the line shape evolution of the H$^{\epsilon 2}$/H48 resonance shown in Figure 3 agrees with the temperature-
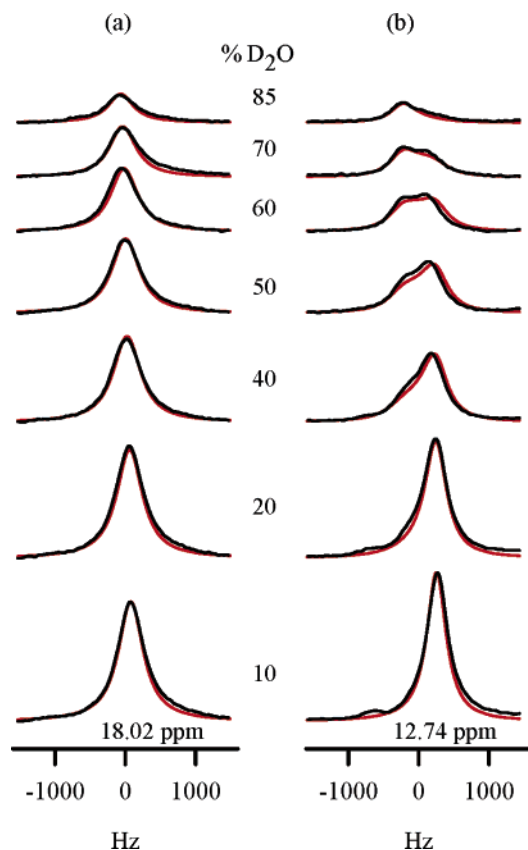
FIGURE 5: Overlay of ¹H NMR experimental data (black) recorded at 285 K and line shape simulation results (red) for the resonances of (a) $H^{\delta 1}$/H48 (centered at 18.02 ppm) and (b) $H^{\epsilon 2}$/H48 (centered at 12.74 ppm) in different H_2O/D_2O solvent mixtures. The simulation incorporates deuterium fractionation factors to account for the change in the overall ¹H signal intensity and the relative distribution of the doublets.

dependent behavior of the exchange rate k_{ex} of $H^{\delta 1}$/H48, which has been determined previously through the Arrhenius plot of the temperature effect on its resonance line width (*6*). A notable feature for an equally populated two-state chemical exchange is the coalescent point, at which the top of the line shape is flat. At such a point the exchange rate is given by

$$k_{coalescence} = \frac{2\pi(\nu_A - \nu_B)}{2\sqrt{2}} \quad (2)$$

where ν_A and ν_B are the Lamor frequencies in hertz of the two sites (*19*). With roughly 0.13 ppm or 78 Hz of chemical shift difference for the $H^{\epsilon 2}$/H48 spin (Figure 5b), $k_{coalescence}$ is calculated to be around 173 Hz, which corresponds to 293.9 K if the isotope effect is attributed to H/D exchange at the $H^{\delta 1}$/H48 site (*6*). In agreement with this estimation, the coalescence temperature can be easily identified to be around 292.9 K in Figure 3 since protium and deuterium are close to being equally populated at the $N^{\delta 1}$/H48 site for the sample used. Therefore, it can be inferred from resonance shifts upon deuteration that the slightly upfield resonance of $H^{\epsilon 2}$ arises from the $N^{\delta 1}-H$ chemical environment, whereas the slightly downfield one is attributed to the $N^{\delta 1}$-D situation.

In contrast, no split was visible for the peak of $H^{\delta 1}$/H48 at 18 ppm (Figure 5a). Only a slight downfield shift can be discerned with increasing deuterium content, which indicates

a faster H/D exchange at the $N^{\epsilon 2}$/H48 position and/or a smaller indirect isotope effect defined as $^4\Delta^1H$-$\delta 1(N^{\epsilon 2}$-D).

Quantitative Line Shape Analysis. Line shape analyses were performed to confirm the cross-modulation as well as to extract the quantitative assessment of the secondary isotope effect on chemical shifts for both spins. The formalism follows a modified Bloch equation known as the McConnell equation that describes a two-state exchange process (*19, 20*). In the subsequent derivation the subscripts of "H" and "D" refer to H and D spin attached to $N^{\delta 1}$/H48, respectively. Assuming $H^{\epsilon 2}$/H48 experiences a chemical exchange between $N^{\delta 1}$-H and $N^{\delta 1}$-D states with parameters of mean lifetime (τ_H and τ_D), Larmor precession angular frequency (ω_H and ω_D), and fractional population (P_H and P_D), the line shape can be derived from solving the McConnell equation:

$$\frac{dG_H}{dt} + \alpha_H G_H = -i\gamma H_1 M_{0H} + \frac{G_D}{\tau_D} - \frac{G_H}{\tau_H} \quad (3)$$

$$\frac{dG_D}{dt} + \alpha_D G_D = -i\gamma H_1 M_{0D} + \frac{G_H}{\tau_H} - \frac{G_D}{\tau_D} \quad (4)$$

$$\alpha_H = \frac{1}{T_{2H}} - i(\omega_H - \omega) \quad (5)$$

$$\alpha_D = \frac{1}{T_{2D}} - i(\omega_D - \omega) \quad (6)$$

where G is the transverse complex moment, M_0 is the macroscopic equilibrium moment, H_1 is the oscillating field, γ is the gyromagnetic ratio, and T_2 is the transverse relaxation time.

By setting the slow passage condition

$$\frac{dG_H}{dt} = \frac{dG_D}{dt} = 0 \quad (7)$$

the total complex moment is obtained:

$$G = G_H + G_D =$$

$$-i[\gamma H_1(M_{0H} + M_{0D})]\left[\frac{\tau_H + \tau_D + \tau_H\tau_D(\alpha_H P_D + \alpha_D P_H)}{(1 + \alpha_H\tau_H)(1 + \alpha_D\tau_D) - 1}\right] \quad (8)$$

The first bracket in G is a real number proportional to the intensity of the observable NMR signal. Unlike most other simulations (*19*), M_0 in this work, the sum of M_{0H} and M_{0D}, is not a constant but determined by the population of protium attached to $N^{\epsilon 2}$/H48. Thus the peak intensity is a function of parameter $\phi^{\epsilon 2}$ and variable x:

$$\text{intensity} \propto \gamma H_1 M_0 = f(\phi^{\epsilon 2}, \chi) \quad (9)$$

By incorporating eq 1, the following equation is obtained for the overall signal intensity:

$$I^{\epsilon 2} = f(\phi^{\epsilon 2}, \chi) = \frac{I^{\epsilon 2}_{max} x}{\phi^{\epsilon 2}(1 - x) + x} \quad (10)$$

On the other hand, the second bracket in eq 8 is a complex function. It describes the relative magnitude of the $H^{\epsilon 2}$/H48 doublet, which is modulated by the relative population of

H/D on the $N^{\delta 1}$/H48 site as a function of $\phi^{\delta 1}$ and variable x:

$$\text{shape} \propto \frac{\tau_H + \tau_D + \tau_H\tau_D(\alpha_H P_D + \alpha_D P_H)}{(1 + \alpha_H \tau_H)(1 + \alpha_D \tau_D) - 1} = f(\phi^{\delta 1}, \chi) \quad (11)$$

Due to the correlation between the fractional population and the mean lifetime, the following relationships can be established for $N^{\delta 1}$-H and $N^{\delta 1}$-D:

$$P_H = \frac{\tau_H}{\tau_H + \tau_D} = \frac{x}{\phi^{\delta 1}(1 - x) + x} \quad (12)$$

$$P_D = \frac{\tau_D}{\tau_H + \tau_D} = \frac{\phi^{\delta 1}(1 - x)}{\phi^{\delta 1}(1 - x) + x} \quad (13)$$

which in turn leads to the ratio:

$$\frac{\tau_H}{\tau_D} = \frac{P_H}{P_D} = \frac{x}{\phi^{\delta 1}(1 - x)} \quad (14)$$

Thus we can set

$$\tau_H = x\tau \quad (15)$$

$$\tau_D = \phi^{\delta 1}(1 - x)\tau \quad (16)$$

where τ is a generalized lifetime.

By incorporating eqs 10, 12, 13, 15, and 16 into eq 8, a final equation of G is obtained whose imaginary part describes the observable NMR signal of $H^{\epsilon 2}$/H48 spin—the evolution of line shape as well as the change of overall ^{1}H resonance intensity at different H_2O/D_2O mixtures:

$$G = -i\frac{I^{\epsilon 2}_{max} x}{\phi^{\epsilon 2}(1 - x) + x} \times$$
$$\left(\frac{x\tau + \phi^{\delta 1}(1 - x)\tau + x\phi^{\delta 1}(1 - x)\tau^2\left(\frac{\alpha_H \phi^{\delta 1}(1 - x) + \alpha_D x}{\phi^{\delta 1}(1 - x) + x}\right)}{(1 + \alpha_H x\tau)(1 + \alpha_D \phi^{\delta 1}(1 - x)\tau) - 1}\right)$$
$$(17)$$

To simplify the simulation, it is assumed that $T_{2,H} = T_{2,D} = T_2$. As a starting point, the generalized lifetime τ of $H^{\delta 1}$/H48 was estimated from its k_{ex} at 285 K ($\sim$12.5 ms), the transverse relaxation time T_2 of $H^{\epsilon 2}$/H48 from its signal line width at 10% D_2O ($\sim$5.6 ms), and the chemical shift difference of the $H^{\epsilon 2}$ doublet from the peak (10% D_2O) to peak (85% D_2O) difference in Figure 5b ($\sim$0.13 ppm). The deuterium fractionation factors ($\phi^{\epsilon 2}$ and $\phi^{\delta 1}$) of both spins have been presented above. After several rounds of iteration a set of parameters was obtained (Table 1) that can generally reproduce the major experimental features, i.e., the changes in shape and magnitude (Figure 5b). The work on the simulation of the $H^{\delta 1}$/H48 peak was performed essentially in the same way (Figure 5a, Table 1).

Unusual Four-Bond Secondary Isotope Effect Supports a Strong Hydrogen Bond. It is significant that $H^{\delta 1}$/H48 induces a three times larger secondary isotope effect on $H^{\epsilon 2}$/H48 than vice versa, which could be regarded as additional evidence in support of a stronger hydrogen bond between H48 and the TSA. The effect implicating a change in the shielding

Table 1: Summary of Line Shape Simulation on Bovine Pancreatic sPLA$_2$ in the Presence of TSA

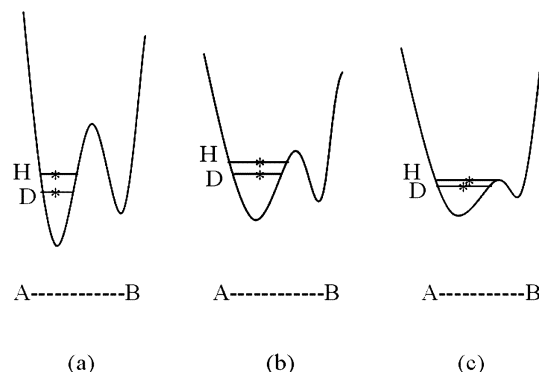| parameter	$H^{\epsilon 2}$/H48 (12.67 ppm) line shape simulation	$H^{\delta 1}$/H48 (18.00 ppm) line shape simulation
indirect isotope effect (ppm)	$^4\Delta^1$H-$\epsilon 2(N^{\delta 1}$-D) $\sim$ -0.15	$^4\Delta^1$H-$\delta 1(N^{\epsilon 2}$-D) $\sim$ -0.05
H/D fractionation factor ($\phi^{\delta 1}$)	$\sim$0.60	$\sim$0.60
H/D fractionation factor ($\phi^{\epsilon 2}$)	$\sim$0.95	$\sim$0.95
lifetime τ (ms)	$\sim$22	$\sim$15
T_2 (ms)	$\sim$6.67	$\sim$4.76

FIGURE 6: Schematic diagrams of bridging proton potential curves. Horizontal lines indicate the zero-point vibrational energy levels, and asterisks mark the equilibrium positions of protium and deuterium. (a) In a normal hydrogen bond, the equilibrium positions of H and D will not be very different. (b) Lower fractionation factor can be indicative of a widened potential function. (c) Larger intrinsic isotope effect implicates higher anharmonicity in the ground vibrational state. A and B represent the two heteroatoms.

might be indicative of a positional change of protons and will be discussed in relation to the concerted proton-relay mechanism in sPLA$_2$.

It is known that due to the anharmonicity of the effective vibrational potential and the lower zero-point energy of deuterium, the N−D bond is shorter than its corresponding N−H bond (*21*), e.g., by 0.01 Å as predicted in the hydrated ammonium ion (*22*). For the prevalent weak hydrogen bonds with double minimum function, the proton is located in the bottom of one of the nearly symmetrical potential wells where the anharmonicity is low. Thus the equilibrium positions of protium and deuterium will not be very different, and the deuterium effect on chemical shifts will be small. In this case, even the primary effect $\Delta[\delta_H - \delta_D]$ could be negligible (*23*). When the hydrogen bond becomes stronger, the effective vibrational potential well of the bridging atom becomes broader with a corresponding increase in anharmonicity, and the bridging atom, either hydrogen or deuterium, will be approaching to the top of the barrier in the double minimum potential well where the anharmonicity is significantly larger (Figure 6) (*23*). Under such a scenario, the average N−D bond will be shortened to a larger extent with respect to its N−H bond, resulting in a more significant change of molecular geometry via H/D substitution (*23*). Since H48 in sPLA$_2$ was found in a protonated form when complexed with TSA and both imidazole nitrogen atoms act as a donor in their respective hydrogen bonds, the shortening of the H48−TSA hydrogen bond upon deuteration on $N^{\delta 1}$/H48 would push the other bridging proton $H^{\epsilon 2}$ toward the midpoint between the participating heteroatoms in a remi-

niscence of proton relay. As a consequence, $H^{\epsilon 2}$ will be less shielded and hence move downfield in ^1H NMR as shown by the secondary isotope effect, whereas the $^2H^{\delta 1}$/H48 like other bridging protons in LBHB is predicted to experience higher shielding and move upfield resulting in the primary isotope effect.

Another comparison in support of the above interpretation came from parallel fractionation factor experiments performed on free sPLA$_2$ under acidic condition, where H48 exists in the imidazolium form (*6*). First, no visible splitting can be observed for the $H^{\epsilon 2}$/H48 signal with various D_2O/H_2O solvent mixtures (Figure 2c,d). Second, while the peak does show a slightly downfield shift with increasing D_2O/H_2O ratio, the H/D isotope effect is estimated to be ca. 0.05 ppm only.

The fractionation factor $\phi^{\epsilon 2}$ was determined to be around 1.14 in the protonated H48 of free sPLA$_2$ (Figure 4b). The comparable size to that of $H^{\epsilon 2}$/H48 in the presence of TSA suggests that the hydrogen bond between D99 and H48 remains weak regardless of the hydrogen bond type for which $N^{\delta 1}$/H48 is engaged in. It has been postulated that D99 is critical for proton extraction and/or charge stabilization in sPLA$_2$ catalysis. In this work, accompanying the proton relay that mimics the reaction pathway is the charge transfer. The chemical shift of $H^{\epsilon 2}$/H48, ranging from 11.46 ppm (neutral ring) to 13.02 ppm (+1 charged ring), has been found in good correlation with the charge on the H48 imidazole ring (*6*). Thus a downfield shift of 0.15 ppm for $H^{\epsilon 2}$ indicates around 10% positive charge transfer to the imidazole ring upon deuteration on the $N^{\delta 1}$/H48.

Use of the Secondary H/D Isotope Effect To Probe Hydrogen Bond Strength. There are two types of deuterium-induced isotope effects: equilibrium and intrinsic ones. The H/D fractionation factor belongs to the equilibrium effect, which is mainly attributed to mass effects on zero-point energies. The intrinsic effect includes primary and secondary isotope effects on chemical shifts, which arise from changes of molecular geometries via deuterium substitution, e.g., changes in the bond length and/or bond angle (Figure 6). In principle, these correlated but nonredundant effects taken together will provide information on the nature of a bridging proton's vibrational potential, i.e., the magnitude of the harmonic force constant as well as the degree of anharmonicity.

One of the intrinsic H/D isotope effects in association with strong hydrogen bonds is the large primary deuterium isotope effect on the chemical shift of the bridging proton: $\Delta[\delta_H - \delta_D] = 0.5-0.9$ ppm (*3, 23*). While such an effect has been observed in serine protease by recording both ^1H and ^2H NMR spectra (*12*), lower sensitivity and quadrupolar line broadening of the ^2H signal makes this type of measurement very difficult with a biological sample. In the present study, attempts to observe the $^2H^{\delta 1}$/H48 signal in the ^2H NMR recorded on the sPLA$_2$−TSA sample dissolved in 100% D_2O were not successful within a reasonable time frame (30000 transients in more than 10 h experimental time). An alternative approach would be either to measure the radioactive tritium isotope effect (*24*) or to use another reporter nucleus, such as ^1H, ^{13}C, and ^{15}N spins, to investigate the secondary isotope effect of the same origin to identify hydrogen bond type. In the present system the latter can be readily analyzed from ^1H NMR, and an internal reference is

available for comparison. In a more complicated situation, ^{13}C/^{15}N isotope labeling and 2D heteronuclear correlation NMR experiments would be necessary.

The intrinsic H/D secondary isotope effect on hyperfine chemical shifts has been observed with small organic molecules at low temperatures (*25, 26*), with DNA (*13, 14, 27*), and with some paramagnetic proteins (*28, 29*). Although these effects were generally correlated with hydrogen bond strength, this is the first report, to the best of our knowledge, that a prominent secondary four-bond H/D isotope effect on the ^1H chemical shift is observed in a protein. The result could bear significant insight on the catalytic mechanism of the enzyme. In conclusion, this observation together with other spectroscopic observations such as extremely low-field proton signal points to an unusual magnetic environment of the $H^{\delta 1}$/H48 proton, indicative of a strong intermolecular hydrogen bond in the complex. However, it still remains unanswered how these unusual physicochemical properties can be quantitatively correlated with the magnitude of the hydrogen bond energy that has direct biological relevance to enzymatic catalysis. An extended theoretical work would be required to understand the relationship (*30, 31*), and the information learned from experimental and theoretical studies should provide more insights into the nature and physiological role of hydrogen bonding in biological systems.

REFERENCES

1. Yuan, C., and Tsai, M.-D. (1999) Pancreatic phospholipase A(2): new views on old issues, *Biochim. Biophys. Acta 1441*, 215−222.
2. Frey, P. A., Whitt, S. A., and Tobin, J. B. (1994) A low-barrier hydrogen bond in the catalytic triad of serine proteases, *Science 264*, 1927−1930.
3. Frey, P. A. (2004) Strong hydrogen bonding in chymotrypsin and other serine proteases, *J. Phys. Org. Chem. 17*, 511−520.
4. Ash, E. L., Sudmeier, J. L., De Fabo, E. C., and Bachovchin, W. W. (1997) A low-barrier hydrogen bond in the catalytic triad of serine proteases? Theory versus experiment, *Science 278*, 1128−1132.
5. Scott, D. L., Otwinowski, Z., Gelb, M. H., and Sigler, P. B. (1990) Crystal structure of bee-venom phospholipase A2 in a complex with a transition-state analogue, *Science 250*, 1563−1566.
6. Poi, M. J., Tomaszewski, J. W., Yuan, C., Dunlap, C. A., Andersen, N. H., Gelb, M. H., and Tsai, M.-D. (2003) A low barrier hydrogen bond between histidine of secreted phospholipase A2 and a transition state analog inhibitor, *J. Mol. Biol. 329*, 997−1009.
7. Mildvan, A. S., Harris, T. K., and Abeygunawardana, C. (1999) Nuclear magnetic resonance methods for the detection and study of low-barrier hydrogen bonds on enzymes, *Methods Enzymol. 308*, 219−245.
8. Yu, L., and Dennis, E. A. (1991) Critical role of a hydrogen bond in the interaction of phospholipase A2 with transition-state and substrate analogues, *Proc. Natl Acad. Sci. U.S.A. 88*, 9325−9329.
9. Frey, P. A. (2001) Strong hydrogen bonding in molecules and enzymatic complexes, *Magn. Reson. Chem. 39*, S190−S198.
10. Markley, J. L., and Westler, W. M. (1996) Protonation-state dependence of hydrogen bond strengths and exchange rates in a serine protease catalytic triad: bovine chymotrypsinogen A, *Biochemistry 35*, 11092−11097.
11. Lin, J., Westler, W. M., Cleland, W. W., Markley, J. L., and Frey, P. A. (1998) Fractionation factors and activation energies for exchange of the low barrier hydrogen bonding proton in peptidyl trifluoromethyl ketone complexes of chymotrypsin, *Proc. Natl. Acad. Sci. U.S.A. 95*, 14664−14668.
12. Cassidy, C. S., Lin, J., and Frey, P. A. (2000) The deuterium isotope effect on the NMR signal of the low-barrier hydrogen bond in a transition-state analog complex of chymotrypsin, *Biochem. Biophys. Res. Commun. 273*, 789−792.
13. Vakonakis, I., Salazar, M., Kang, M., Dunbar, K. R., and LiWang, A. C. (2003) Deuterium isotope effects and fractionation factors

of hydrogen-bonded A:T base pairs of DNA, *J. Biomol. NMR 25*, 105−112.

14. Vakonakis, I., and LiWang, A. C. (2004) Trans-hydrogen bond deuterium isotope effects of A:T base pairs in DNA, *J. Biomol. NMR 29*, 65−72.

15. Hansen, P. E. (2000) Isotope effects on chemical shifts of proteins and peptides, *Magn. Reson. Chem. 38*, 1−10.

16. Noel, J. P., Bingman, C. A., Deng, T. L., Dupureur, C. M., Hamilton, K. J., Jiang, R. T., Kwak, J. G., Sekharudu, C., Sundaralingam, M., and Tsai, M. D. (1991) Phospholipase A2 engineering. X-ray structural and functional evidence for the interaction of lysine-56 with substrates, *Biochemistry 30*, 11801−11811.

17. Plateau, P., and Gueron, M. (1982) Exchangeable proton NMR without base-line distortion, using new strong-pulse sequences, *J. Am. Chem. Soc. 104*, 7310−7311.

18. Yuan, C., Byeon, I. J., Li, Y., and Tsai, M.-D. (1999) Structural analysis of phospholipase A2 from functional perspective. 1. Functionally relevant solution structure and roles of the hydrogen-bonding network, *Biochemistry 38*, 2909−2918.

19. Bain, A. D. (2003) Chemical exchange in NMR, *Prog. Nucl. Magn. Reson. Spectrosc. 43*, 63−103.

20. Pople, J. A., Schneider, W. G., and Bernstein, H. J. (1959) *High-resolution Nuclear Magnetic Resonance*, McGraw-Hill, New York.

21. Dziembowska, T., and Rozwadowski, T. (2001) Application of the deuterium isotope effect on NMR chemical shift to study proton-transfer equilibrium, *Curr. Org. Chem. 5*, 289−313.

22. Munch, M., Hansen, A. E., Hansen, P. E., and Bouman, T. D. (1992) Ab initio calculations of deuterium-isotope effects on hydrogen and nitrogen nuclear magnetic shielding in the hydrated ammonium ion, *Acta Chem. Scand. 46*, 1065−1071.

23. Hibbert, F., and Emsley, J. (1990) Hydrogen bonding and chemical reactivity, *Adv. Phys. Org. Chem. 26*, 255−379.

24. Westler, W. M., Frey, P. A., Lin, J., Wemmer, D. E., Morimoto, H., Williams, P. G., and Markley, J. L. (2002) Evidence for a strong hydrogen bond in the catalytic dyad of transition-state analogue inhibitor complexes of chymotrypsin from proton-triton NMR isotope shifts, *J. Am. Chem. Soc. 124*, 4196−4197.

25. Smirnov, S. N., Golubev, N. S., Denisov, G. S., Benedict, H., Schah-Mohammedi, P., and Limbach, H. H. (1996) Hydrogen−deuterium isotope effects on the NMR chemical shifts and geometries of intermolecular low-barrier hydrogen-bodned complexes, *J. Am. Chem. Soc. 118*, 4094−4101.

26. Schah-Mohammedi, P., Shenderovich, I. G., Detering, C., Limbach, H. H., Tolstoy, P. M., Smirnov, S. N., Denisov, G. S., and Golubev, N. S. (2000) Hydrogen/deuterium-isotope effects on NMR chemical shifts and symmetry of homoconjugated hydrogen-bonded ions in polar solution, *J. Am. Chem. Soc. 122*, 12878−12879.

27. Vakonakis, I., and LiWang, A. C. (2004) N1···N3 hydrogen bonds of A:U base pairs of RNA are stronger than those of A:T base pairs of DNA, *J. Am. Chem. Soc. 126*, 5688−5689.

28. Lee, K. B., McLachlan, S. J., and La Mar, G. N. (1994) Hydrogen isotope effects on the proton nuclear magnetic resonance spectrum of bovine ferricytochrome b5: axial hydrogen bonding involving the axial His-39 imidazole ligand, *Biochim. Biophys. Acta 1208*, 22−30.

29. Xia, B., Wilkens, S. J., Westler, W. M., and Markley, J. L. (1998) Amplification of one-bond H-1/H-2 isotope effects on N-15 chemical shifts in *Clostridium pasteurianum* rubredoxin by Fermi-contact effects through hydrogen bonds, *J. Am. Chem. Soc. 120*, 4893−4894.

30. Garcia-Viloca, M., Gelabert, R., Gonzalez-Lafont, A., Moreno, M., and Lluch, J. M. (1997) Is an extremely low-field proton signal in the NMR spectrum conclusive evidence for a low-barrier hydrogen bond?, *J. Phys. Chem. A 101*, 8727−8733.

31. Molina, P. A., and Jensen, J. H. (2003) A predictive model of strong hydrogen bonding in proteins: the $N^{\delta 1}-H-O^{\delta 1}$ hydrogen bond in low-pH α-Chymotrypsin and α-Lytic protease, *J. Phys. Chem. B 107*, 6226−6233.